Energy Localization in Photonic Crystals of a Purely Nonlinear Origin

Claudio Conti,* Stefano Trillo,† and Gaetano Assanto*

National Institute for the Physics of Matter, INFM-RM3, Via della Vasca Navale 84, 00146 Roma, Italy

(Received 12 April 2000)

We investigate electromagnetic localization in a *nonlinear* photonic crystal, i.e., a structure with a stop band in its nonlinear spectral response. Taking a one-dimensional model of degenerate two-wave interaction we introduce the concept of parametric *nonlinear-gap* solitons, that is, strongly localized two-color locked envelopes arising from interplay of two nonlinear effects, which propagate slowly. We discuss the observable signature of these novel localized structures.

PACS numbers: 42.70.Qs, 42.65.Pc, 42.65.Tg

There is a growing interest in band gap materials or *"photonic crystals"* (PCs [1]) and their 1D analogs such as Bragg gratings [2,3]. A universal feature of periodic media or discrete chains which exhibit stop bands (gaps) in their *linear* dispersion relation, is the existence of self-transparent *gap soliton* envelopes supported by the nonlinearity [2–6]. As witnessed by excellent experimental results [7], nonlinear optics is a privileged observatory for these phenomena. On the other hand also *nonlinear* PCs with *homogeneous linear properties* have been proposed [8], generalizing the concept of quasi-phase-matching (QPM) of parametric interactions [9]. So far, the role of QPM was investigated in relation to trapping of nondiffractive tranverse wave packets [10]. Conversely, the basic question we address in this Letter is *whether a nonlinear PC can sustain solitary structures, strongly localized along the propagation direction*, reminiscent of linear-gap solitons. Based on intuition, one could think that such a possibility is prevented by the absence of the damping due to a low-power stop band, which ensures the correct exponential decay along soliton tails. On the contrary, by specifically focusing on the example of 1D backward second-harmonic generation (BSHG) [11–14], we predict dramatic localization and self-transparency effects, owing to formation of solitons due to a *nonlinear stop band*, i.e., nonlinear-gap solitons (NGS). These NGS are self-induced in a nonlinear PC which stems from BSHG, through the unavoidable contribution of Kerr nonlinearities. Notice that BSHG is the simplest, experimentally demonstrated [11], prototype of parametric mixing which leads to a nonlinear frequency gap, i.e., power-induced reflection in an otherwise linearly transparent structure. In this respect a BSHG reflector is the nonlinear counterpart of a linear Bragg grating.

Self-induced gap solitons exist in discrete systems, where they are standing kinklike excitations [15]. Our results prove that self-induced NGS of a completely different nature can also propagate in continuous systems. Our fully solvable model shows that these are slowly moving objects which exhibit a strong energy confinement and exist also with vanishing background waves.

Specifically, let us consider a total field $E(Z, T) = E_1(Z,T)\exp(ik_1Z - i\omega_0 t) + E_2(Z,T)\exp(-ik_2Z - i2\omega_0 t)$, where $k_l = k(l\omega_0)$, $l = 1, 2$, propagating in a nonlinear $\chi^{(2)}$ grating with stepwise changes along the Z axis. The forward- and backward-propagating envelopes E_1 and E_2, at the fundamental frequency (FF) and its second-harmonic (SH), respectively, obey the system

$$\begin{aligned} L_1E_1 + \chi_2(Z)E_2E_1^* e^{i\Delta kZ} + \\ (\tilde{X}_1|E_2|^2 + \tilde{S}_1|E_1|^2)E_1 = 0, \\ L_2E_2 + \chi_2(Z)E_1^2 e^{-i\Delta kZ} + \\ (\tilde{X}_2|E_1|^2 + \tilde{S}_2|E_2|^2)E_2 = 0, \end{aligned} \tag{1}$$

where $L_1 = iV_1^{-1}\partial_T + i\partial_Z$, $L_2 = iV_2^{-1}\partial_T - i\partial_Z$, $V_l = dk/d\omega|^{-1}_{l\omega_0}$, $l = 1, 2$, are group velocities, $\Delta k = \Delta k(\omega_0) = k_2 + 2k_1$ is the wave vector mismatch, and Fourier expansion of $\chi^{(2)}$ yields $\chi_2(Z) = \hat{\chi}_2 \sum_{m\neq 0}\exp(im2\pi Z/\Lambda)$. For a grating pitch $\Lambda = 2m\pi/\Delta k(\omega_0)$, perfect BSHG phase matching is achieved at ω_0 with a suitable integer m, and Eqs. (1) are conveniently recast in a dimensionless form as

$$\begin{aligned} i(\partial_t + \partial_z)u_1 + u_2u_1^* + (X_1'|u_2|^2 + S_1'|u_1|^2)u_1 = 0, \\ i(v^{-1}\partial_t - \partial_z)u_2 + \frac{u_1^2}{2} + (X_2'|u_1|^2 + S_2'|u_2|^2)u_2 = 0, \end{aligned} \tag{2}$$

where $u_l = \sqrt{2}E_l/\sqrt{lI_r}$, $t = V_1T/Z_{nl}$, $z = Z/Z_{nl}$, $Z_{nl} = 1/(\hat{\chi}_2\sqrt{I_r})$ being a nonlinear length scale associated with a reference intensity I_r, and $v = V_2/V_1$. The normalized cubic coefficients $S_l' = l(\tilde{S}_l + \hat{S}_l)\sqrt{I_r}/(2\hat{\chi}_2)$ and $X_l' = (\tilde{X}_l + \hat{X}_l)\sqrt{I_r}/(l\hat{\chi}_2)$, with $l = 1, 2$ account for the effective corrections $\hat{S}_l$, $\hat{X}_l$ to the intrinsic (i.e., material) Kerr coefficients $\tilde{S}_l, \tilde{X}_l$, which arise unavoidably from the quadratic grating [10].

Neglecting for the time being the cubic terms in Eqs. (2), pure BSHG is responsible of the appearance of an *intrinsically nonlinear* stop band. This is visible in Fig. 1, which shows the output intensity fraction T of a continuous wave (cw) detuned excitation $u_1(0, t) = \exp(-i\delta\omega t)$ at FF versus mismatch $\delta k_0 = 2\delta\omega(1 + v)/v$ (i.e., first order

 0031-9007/00/85(12)/2502(4)$15.00

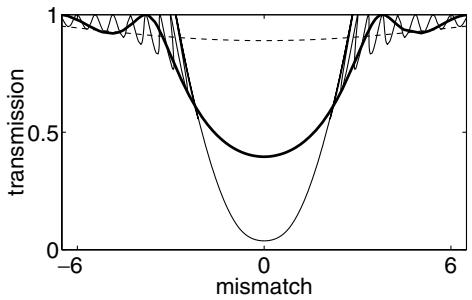

FIG. 1. Transmitted intensity fraction T versus mismatch $\delta k_0 = 2\delta\omega(1+v)/v$ in a BSHG reflector of length L in the quasilinear regime ($z_L = L/Z_{nl} = 0.5$, dashed curve), intermediate ($z_L = 2$, thick solid curve), and high fluences ($z_L = 10$, thin solid curve).

expansion of $k_2 + 2k_1$ around ω_0) for a fixed BSHG reflector length $Z = L$ and increasing fluences (larger values of $z_L = L/Z_{nl}$). At relatively low fluences, the transmission T is high and spectrally flat (see dashed line), whereas higher powers give rise to enhanced back conversion to SH beam at frequency $2\delta\omega$, which in turn results into a *bistable* response with a stop band centered at phase matching (see thin solid curve in Fig. 1).

Our goal is to show that the unavoidable cubic contributions bleach the nonlinear reflection, inducing self-transparency effects mediated by strongly localized envelopes (solitons) slowly moving at normalized velocity V. To this end, we seek two-parameter $(V, \delta\omega)$ traveling waves of the form

$$u_1 = \sqrt{(1-V)(1+V/v)}\,u(\zeta)\exp[i\delta\omega(z-t)],$$
$$u_2 = (1-V)w(\zeta)\exp[i2\delta\omega(z-t)],$$

where $\zeta = z - Vt$, and u, w obey the system

$$-i\dot{u} = wu^* + X_1|w|^2u + S_1|u|^2u,$$
$$i\dot{w} = \delta k w + \frac{u^2}{2} + X_2|u|^2w + S_2|w|^2w, \tag{3}$$

formally identical to the stationary version of Eqs. (2) once we define the rescaled coefficients $X_{1,2} = X'_{1,2}(1-V)$, $S_1 = S'_1(1+V/v)$, and $S_2 = S'_2(1-V)^2/(1+V/v)$. The dot stands for $d/d\zeta$, and $\delta k = \frac{2(1+1/v)\delta\omega}{(1+V/v)}$ is the wave vector mismatch in the soliton frame. Equations (3) can be reduced to an integrable Hamiltonian oscillator by exploiting the conservation of photon flux (i.e., Poynting vector) $P = \frac{|u|^2}{2} - |w|^2$. In terms of the variables $x \equiv |w|\cos\phi$, $y \equiv |w|\sin\phi$, with $\phi \equiv \mathrm{Arg}(w) - 2\mathrm{Arg}(u)$, we obtain

$$\dot{x} = \frac{\partial H}{\partial y}; \qquad \dot{y} = -\frac{\partial H}{\partial x},$$
$$H = x(x^2+y^2+P) + \frac{\Delta}{2}(x^2+y^2) + \frac{\sigma}{4}(x^2+y^2)^2. \tag{4}$$

Here both the overall detuning $\Delta = \delta k + 2(X_2 + 2S_1)P$, and the dephasing term proportional to $\sigma = 2(X_2 + 2S_1) + 2X_1 + S_2$ account for Kerr-induced local modifications of phase matching. Equations (4) can be further reduced, in terms of SH intensity $\eta(\zeta) = x^2 + y^2 = |w(\zeta)|^2$, to a decoupled equation $\ddot{\eta} = -\partial U/\partial\eta$ for the 1D motion of an ideal particle with energy $E = \dot{\eta}^2/2 + U(\eta)$ in a potential well $U(\eta)$ [16]. We obtain $2[U(\eta) - E] = \frac{\sigma^2}{4}\eta^4 + (\sigma\Delta - 4)\eta^3 + (\Delta^2 - 8P + 2H_0\sigma)\eta^2 - 4(P^2 + H_0\Delta)\eta + 4H_0^2$ where H_0 is a particular value of the Hamiltonian (calculated on either input or output section). Solitons correspond to homoclinic loops emanating from the unstable eigenmodes $\eta = \eta_e$, $\phi = \phi_e$ (i.e., $\partial U/\partial\eta|_{\eta_e} = 0$) of Eqs. (4). In order to establish their existence, we have performed a complete bifurcation analysis of Eqs. (4). First, if we drop cubic terms ($\Delta = \delta k$, $\sigma = 0$), two *phase-locked* eigenmodes (i.e., $\phi_e = 0$ for $\delta k < 0$, and $\phi_e = \pi$ for $\delta k > 0$) appear above the bifurcation point $\delta k^2 = 12P$ due to a saddle-node bifurcation which preserves the symmetry $\delta k \to -\delta k$. In this case, the potential $U(\eta)$ is cubic and admits bound (i.e., periodic) or unbound field evolutions separated by the following homoclinic loop

$$|w(\zeta)|^2 = \eta(\zeta) = \eta_e + \kappa_1[\tanh^2(\sqrt{\kappa_1}\,\zeta) - 1], \tag{5}$$

where $4\kappa_1 = \sqrt{\delta k^4 - 48H_e\delta k - 16\delta k^2P + 16P^2}$, $H_e = H(\eta_e, \phi_e)$, and $\eta_e = [\delta k^2 - 6P + \sqrt{\delta k^2(\delta k^2 - 12P)}]/18$ is the asymptotic value. Equation (5) describes moving parametric dark solitons: the intensity profiles $|w(\zeta)|^2$ and $|u(\zeta)|^2 = 2(P + |w(\zeta)|^2)$ show a dip at $\zeta = 0$ accompanied by a phase kink $\phi(\zeta)$ [with $\phi(+\infty) - \phi(-\infty) = 2k\pi$, k integer]. Importantly, from this analysis we draw the conclusion that no energy localization occurs in pure BSHG.

However, cubic terms in Eqs. (4) break the symmetry of the system, qualitatively altering the bifurcation picture with the birth of a third phase-locked eigenmode from a secondary saddle node. In this case the potential $U(\eta)$ is a double well and homoclinic orbits become double loops separating different domains of bound motion in phase space. In the parameter plane $\Delta - P$ (without loss of generality we set $\sigma = 1$, equivalent to rescale $(\eta, P) \to \sigma^2(\eta, P)$, $\Delta \to \sigma\Delta$, $\zeta \to \zeta/\sigma$) these homoclinic loops exist in the shaded regions B and C of Fig. 2. Although the separatrices differ qualitatively in the two existence domains (see insets in Fig. 2), in both cases the loop encircling the origin describes only a deformation of the dark-dark soliton (5). Conversely, the outer loops represent NGS with *strongly localized* bright envelopes on a cw background (pedestal)

$$|w(\zeta)|^2 = \frac{\eta_e + \kappa_2\,\mathrm{sech}(\sqrt{\kappa_1}\,\zeta)}{1 + \kappa_3\,\mathrm{sech}(\sqrt{\kappa_1}\,\zeta)};$$
$$|u(\zeta)|^2 = 2(|w|^2 + P), \tag{6}$$

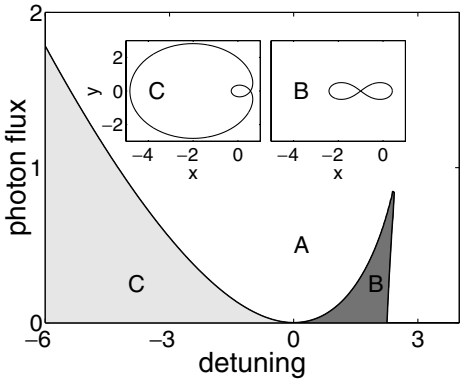

FIG. 2. Existence map of localized envelopes of Eqs. (4) in the parameter plane $\Delta - P$ ($\sigma = 1$, see text). Insets B and C display homoclinic trajectories in the phase plane (x, y), and represent localized waves in the corresponding shaded regions. In A (blank region) no solitary waves exist.

with $4\kappa_1 = (\eta_1 - \eta_2)(\eta_2 - \eta_3)$, $\kappa_2 = [\eta_1\eta_2 + \eta_2\eta_3 - 2\eta_1\eta_3]/[\eta_1 - \eta_3]$, and $\kappa_3 = [2\eta_2 - \eta_1 - \eta_3]/[\eta_1 - \eta_3]$ expressed as functions of the roots $\eta_1 < \eta_e = \eta_2 < \eta_3$ of the equation $E - U(\eta) = 0$. The localized wave (6) is always accompanied by a phase kink with a cumbersome expression which can be easily derived from Eqs. (3). This unexpected result can have a physical justification: the envelopes are self-confined by the action of the background waves which, sustaining the nonlinear stop band, favor strong reflection of the escaping photons towards the envelope center. In the center, in turn, reflection is bleached by the high local intensity, which locally draws the mixing interaction out of phase matching.

The NGS family can be characterized in terms of pedestal η_e and peak $|w(\zeta = 0)|^2$ intensities. Noteworthy, the energy of NGS is highly localized in a wide range of negative detunings Δ where the pedestal to peak intensity ratio $R_p = \eta_e/|w(\zeta = 0)|^2$ remains small [see Fig. 3(a)]. Remarkably, in the symmetric case $P = 0$, the pedestal vanishes at phase matching $\Delta = \delta k = 0$ (i.e., nonlinear-gap center; see Fig. 1). In this case, despite the fact that the saddle and homoclinic orbit disappear (the linearization around the origin yields a doubly degenerate zero eigenvalue), the following localized NGS still exist

$$u = \sqrt{2}\,A(\zeta)\exp[ia_u\psi(\zeta)]; \qquad w = -A(\zeta)\exp[ia_w\psi(\zeta)], \tag{7}$$

which has a Lorentzian (i.e., nonhyperbolic) bright-bright intensity profile $A^2(\zeta) = (4/\sigma)^2[1 + (4\zeta/\sigma)^2]^{-1}$, and a phase kink $\psi(\zeta) = \tan^{-1}[(4\zeta/\sigma)]$ of amplitude $a_u = -1 + \frac{4}{\sigma}(X_1 + 2S_1)$ and $a_w = 1 - \frac{4}{\sigma}(2X_2 + S_2)$ [in this case $\phi(+\infty) - \phi(-\infty) = \pi$; see also Fig. 4(b)].

We also emphasize that these parametric NGS are slow waves, i.e., $-\upsilon < V < 1$, meaning that they can travel in the forward or backward directions with physical velocity smaller than V_1 or V_2, respectively. The higher the velocity in the forward (backward) direction, the stronger the FF (SH) soliton component. This is evident from Fig. 3(b), where we plot the FF intensity fraction $R_{FF} = |u_1(0)|^2/(|u_1(0)|^2 + 2|u_2(0)|^2)$ against soliton velocity V, for different values of $\upsilon = V_2/V_1$.

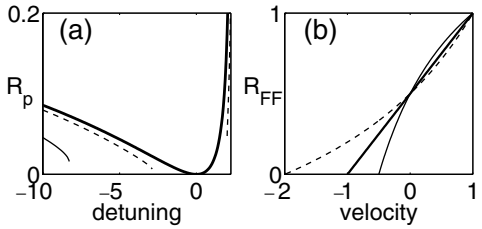

FIG. 3. Features of NGS: (a) Pedestal to peak ratio R_p versus detuning Δ for $P = 0$ (thick solid), $P = 0.5$ (dashed), $P = 3$ (thin solid). (b) Fraction of FF intensity R_{FF} versus V for $P = 0$ and $\upsilon = 1$ (thick solid), $\upsilon = 0.5$ (thin solid), $\upsilon = 2$ (dashed).

Having established the existence of localized waves in a nonlinear PC, one might wonder about their stability. A rigorous theory is challenging and cannot be framed in the usual gap stability problem [17] essentially because in general NGS carry an infinite energy (mass). However, from numerical integration of Eqs. (2), we could ascertain stable propagation in a large portion of the existence domain. This includes stability of the cw background against Hopf bifurcations [12] and modulational instability [when group-velocity dispersions $d^2k/d\omega^2|_{l\omega_0}$, $l = 1, 2$ are included in Eqs. (1) [18]], as it will be reported elsewhere in detail. More importantly, we discuss here the measurable signatures of NGS in a finite nonlinear PC slab $0 < z < z_L$. We choose the boundary condition $u_2(z_L, t) = 0$ consistently with the unidirectional illumination $u_1(0, t) = \sqrt{I_1(t)}$ at FF, and set for definiteness $S'_{1,2} = X'_{1,2} = 0.1$ in Eqs. (2). First, the role of localized states can be gathered from the cw (i.e., $\partial_t = 0$, $I_1 =$ constant) input-output response at FF, namely $|u_1(z_L)|^2$ versus I_1. In Fig. 4 we compare the calculated responses with and without the Kerr contributions. As apparent, the strong reflectivity of pure BSHG at high input fluences is responsible for a dramatic limiting

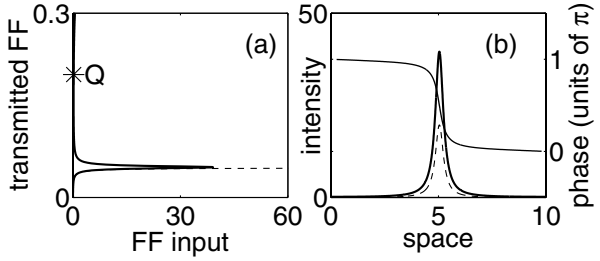

FIG. 4. (a) Transmitted $|u_1(z_L)|^2$ versus cw input FF intensity $I_1 = |u_1(z = 0)|^2$ at phase matching, with (solid) and without (dashed) Kerr effect. (b) Stationary localized intensity profiles at FF (thick solid) and SH (dashed), and phase kink $\phi(\zeta)$ (thin solid), excited at the high-power transparency point Q in (a), within the structure $0 < z < z_L = 10$.

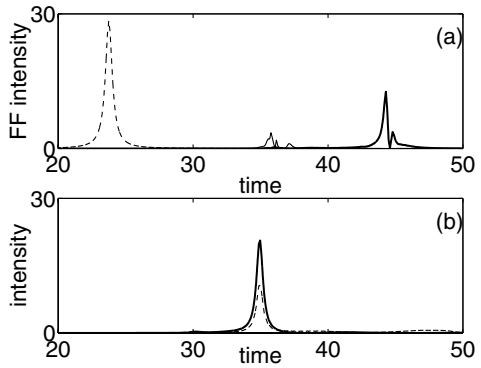

FIG. 5. Pulsed excitation of a slow NGS: (a) temporal profiles of input (dashed) and output intensities without (thin solid) and with (thick solid line) the Kerr contribution; in the latter case the two-hump feature is attributed to weak down conversion from SH to FF which occurs close to the nonlinear-linear boundary at $z_L = 10$ where $u_2(z_L) = 0$. (b) Temporal profiles of SH (solid line) and FF intensities (dashes) in the middle of the structure ($z = 5$).

effect, in turn inhibited by the Kerr effect. The self-transparent state [point Q in Fig. 4(a)] is associated with the excitation of a zero-velocity localized wave, with FF and SH intensity profiles as shown in Fig. 4(b). Similar results are obtained out of phase matching.

Furthermore, we performed numerical experiments to assess the excitability of bright NGS by means of FF pulses. Figure 5 displays a typical result, corresponding to illumination with a Lorentzian chirped pulse [dashed line in Fig. 5(a)] at frequency $\delta\omega = 0$ (nonlinear stop band center $\delta k = 0$; see Fig. 1). In Fig. 5(a) we compare the FF temporal profiles at the output $z = z_L$ in the absence and in the presence of the optical Kerr effect, respectively. While in the former case most of the incident power is up converted to backpropagating SH and only a weak linear FF wave emerges traveling at its linear group velocity ($V = 1$), the Kerr effect dramatically enhances the transmission while inducing a considerable group delay due to the formation of a slow ($V \sim 0.5$) localized pulse. The formation of a NGS is apparent by looking at the snapshot of the two envelope profiles inside the structure ($z = 5$), as shown in Fig. 5(b). The SH beam is locally generated in the backward direction but its envelope, being locked to the FF component, travels forward consistently with soliton features.

Finally, we stress that the reference intensity corresponding to the given value $S'_{1,2} \sim X'_{1,2} \sim 0.1$ (Fig. 5) scales as $I_r \sim 10^{-2}(2\hat{\chi}_2/\tilde{S}_1)^2$ (neglecting QPM correction to $\chi^{(3)}$). For instance, using an order $m \sim 10$ grating [11], we expect I_r in the range of tens of GW/cm^2 in $LiNbO_3$, with a characteristic time scale $T_0 = Z_{nl}/V_1$ of a few ps and $L = z_L Z_{nl} \sim 1$ mm. Such numbers are encouraging for experimental feasibility, but proper engineering of periodic structures [10] and emerging grating technologies [19] allow for significant improvements.

In summary, we have shown that self-induced localized envelopes can propagate in a PC with a nonlinear stop band. Both stationary and slowly moving NGS have a relevant impact on light confinement and self-transparency. These results can be readily generalized to nondegenerate mixing [14] and 1D or 2D [8] nonlinear PCs of different origins. Applications to optical parametric oscillators and cavityless soliton lasers in gain media [13] can be also envisaged.

This work was funded by INFM (PAIS Project 1999).

*Also at Department of Electronic Engineering, Terza University of Rome, Via della Vasca Navale 84, 00146 Roma, Italy.

†Also at Department of Engineering, University of Ferrara, Via Saragat 1, 44100 Ferrara, Italy.

[1] J. D. Joannopoulos, R. D. Meade, and J. N. Winn, Photonic Crystals (Princeton University Press, Princeton, New Jersey, 1995).
[2] W. Chen and D. L. Mills, Phys. Rev. Lett. **58**, 160 (1987).
[3] D. N. Christodoulides and R. I. Joseph, Phys. Rev. Lett. **62**, 1746 (1989); A. B. Aceves and S. Wabnitz, Phys. Lett. A **141**, 37 (1989); C. M. De Sterke and J. E. Sipe, in *Progress in Optics XXXIII,* edited by E. Wolf (Elsevier, Amsterdam, 1994), Chap. III.
[4] D. Barday and M. Remoissenet, Phys. Rev. B **41**, 10 387 (1990).
[5] S. John and N. Akozbek, Phys. Rev. Lett. **71**, 1168 (1993); Phys. Rev. E **57**, 2287 (1998).
[6] C. Conti *et al.,* Phys. Rev. Lett. **78**, 2341 (1997); H. He and P. D. Drummond, Phys. Rev. Lett. **78**, 4311 (1997); T. Peschel *et al.,* Phys. Rev. E **55**, 4730 (1997).
[7] B. J. Eggleton *et al.,* Phys. Rev. Lett. **76**, 1627 (1996); D. Taverner *et al.,* Opt. Lett. **23**, 328 (1998); P. Millar *et al.,* Opt. Lett. **24**, 685 (1999).
[8] V. Berger, Phys. Rev. Lett. **81**, 4136 (1998).
[9] J. A. Armstrong *et al.,* Phys. Rev. **127**, 1918 (1962).
[10] C. B. Clausen *et al.,* Phys. Rev. Lett. **78**, 4749 (1997); **83**, 4740 (1999); O. Bang *et al.,* Opt. Lett. **24**, 7 (1999).
[11] J. U. Kang *et al.,* Opt. Lett. **22**, 862 (1997); X. Gu *et al.,* Opt. Lett. **24**, 127 (1999).
[12] See, e.g., M. Matsumoto and K. Tanaka, IEEE J. Quantum Electron. **31**, 700 (1995); G. D'Alessandro *et al.,* Phys. Rev. A **55**, 3211 (1997).
[13] C. Conti *et al.,* Opt. Lett. **24**, 1139 (1999).
[14] A. Picozzi and M. Haelterman, Opt. Lett. **23**, 1808 (1998); Phys. Rev. E **59**, 3749 (1999).
[15] Y. S. Kivshar, Phys. Rev. Lett. **70**, 3055 (1993); B. Denardo *et al.,* Phys. Rev. Lett. **68**, 1730 (1992); G. Huang and Z. Jia, Phys. Rev. B **51**, 613 (1995).
[16] S. Trillo *et al.,* Opt. Lett. **17**, 637 (1992).
[17] V. I. Barashenkov *et al.,* Phys. Rev. Lett. **80**, 5117 (1998); A. De Rossi *et al.,* Phys. Rev. Lett. **81**, 85 (1998).
[18] P. M. Lushnikov *et al.,* Opt. Lett. **23**, 1650 (1998); M. Yu *et al.,* J. Opt. Soc. B **15**, 607 (1998).
[19] V. Ya. Shur *et al.,* Appl. Phys. Lett. **76**, 143 (2000).